BioSystems 104 (2011) 118–126

Contents lists available at ScienceDirect

BioSystems

journal homepage: www.elsevier.com/locate/biosystems

Influence of aluminum oxide on the prebiotic thermal synthesis of Gly-Glu-(Gly-Glu)$_n$ polymer

Patricio Leyton[a,*], R. Antonio Zárate[b], Sandra Fuentes[b], Carolina Paipa[a], Juan S. Gómez-Jeria[c], Yessica Leyton[d]

[a] Departamento de Ciencias Químicas, Facultad de Ecología y Recursos Naturales, Universidad Andrés Bello (UNAB), Los Fresnos 52, Viña del Mar, Chile
[b] Departamento de Física, Facultad de Ciencias, Universidad Católica del Norte, Casilla 1280, Antofagasta, Chile
[c] Departamento de Química, Facultad de Ciencias, Universidad de Chile, Santiago, Chile
[d] Instituto de Química, Facultad de Ciencias, Laboratorio de Fotofísica y Espectroscopia Molecular, Pontificia Universidad Católica de Valparaíso, Chile

ARTICLE INFO

Article history:
Received 11 August 2010
Received in revised form
16 November 2010
Accepted 20 January 2011

Keywords:
Prebiotic chemistry
Thermal synthesis
Vibrational spectroscopy

ABSTRACT

The effect of the aluminum oxide on the thermal synthesis of the glycine–glutamic acid (Gly-Glu-(Gly-Glu)$_n$ polymer is described. The thermal synthesis in the molten state was carried out in the absence and presence of the oxide. In both cases, the vibrational spectra showed characteristic group frequencies corresponding predominantly to a Gly-Glu-(Gly-Glu)$_n$ sequence in the polymeric structure. The theoretical spectral data support the experimental proposed Gly-Glu-(Gly-Glu)$_n$ sequence for the polymer. The SEM–EDX characterization of the solid phase involved in the thermal synthesis showed that the aluminum oxide participates as a site for nucleation and growth of the polymer, explaining the increase of 25% efficiency in the presence of aluminum oxide. Electrophoresis data show shorter polypeptide chains in the presence of aluminum oxide.

1. Introduction

Nearly 50 years ago, Bernal and Goldschmidt independently proposed that clay minerals could play an important role in both the prebiotic chemistry and the origin of life. Most of the non-catalytic prebiotic studied syntheses use simple molecules such as HCN, HCHO, CO, H_2S and NH_3 as starting materials. Thus, prebiotic reactions proceeding in the absence of catalytic surfaces yield a random mixture of organic compounds as happened in the classic Miller–Urey experiment (Martinez-Meeler et al., 2003; Miller, 1955). A new situation occurs when a molecule establishes an adsorbate–substrate interaction with a surface. In this context, mineral surfaces could establish selectivity over the reactive compounds to form the complex biomolecules and biopolymers that may have originated life.

The prebiotic polymer formation involves both the use of condensation agents or catalysts as other different conditions, such as high pressure and temperature (Fouche and Rohlfing, 1976; Simoneit, 2004) and melting processes (Fouche and Rohlfing, 1976; Harada and Fox, 1958; Rohlfing and MacAlhaney, 1976).

The catalytic efficiency of clay minerals for amino acid dimerization is low relative to salt-induced polymer formation mechanism (SIPF), but their importance in polymer chain growth has been mentioned in recent experimental studies (Bujdák and Rode, 2002; Plankensteiner et al., 2004). If the condensation reactions that have been proposed for prebiotic polymer formation are compared, the SIPF reaction has proven to be applicable to a large variety of amino acids and the geochemical conditions of primitive Earth (Bujdák and Rode, 2002; Napier and Yin, 2006). It seems to be clear from these studies that Gly is the most reactive amino acid in many systems. The formation of Gly_2 products could also spontaneously occur in the presence of clay minerals, and traces of these reaction products are often formed in experiments (Lambert, 2008; Napier and Yin, 2006). Although the influence of mineral surfaces in prebiotic chemistry has been broadly accepted, few investigations have been conducted to determine and explain their role at molecular level in molten state (Lambert, 2008; Rohlfing and MacAlhaney, 1976; Schoonen et al., 2004; Schwartz, 1996).

The surfaces resembling minerals that were likely present on the early earth, are mostly silicates, oxides, and sulfides. Aluminum oxide has been suggested as a model for studying a prebiotic surface similar to meteorites or small cosmic dust grains (Bujdák and Rode, 2001), in this sense the alumina (Al_2O_3) detected in cosmic dust is considered to play an important role in dust formation in oxygen-rich stars (Banerjee et al., 2007; Henning et al., 1995; Nittler et al., 1998).

In this work, the thermal synthesis in the molten state of Gly-Glu-(Gly-Glu)$_n$ polymer in the absence and presence of aluminum oxide was performed in the general frame of evaluating the prebi-

* Corresponding author. Tel.: +56 32 2845195; fax: +56 32 2673082.
E-mail address: pleyton@unab.cl (P. Leyton).

0303-2647/$ – see front matter © 2011 Elsevier Ireland Ltd. All rights reserved.
doi:10.1016/j.biosystems.2011.01.008

otic polymerization by mineral surfaces, mainly conducted from a vibrational spectroscopy point of view.

2. Materials and methods

2.1. Reagents

L-glutamic acid (Calbiochem®, 99.1%); glycine (Calbiochem®, 100.0%); aluminum oxide (Merck®, >99%, 0.063–0.200 mm, basic active, specific surface area approx. 120 m^2/g), glycylglycine (Sigma®, 99%), glutamyl-glutamic acid (Sigma®, 99%) and *N*-glycylglutamic acid (Sigma®, 98%). All reagents were used as received.

2.2. Thermal condensation

Polymeric glycylglutamic acid (Gly-Glu-(Gly-Glu)$_n$) was obtained using a modification of the Harada and Fox method (Harada and Fox, 1958). A reaction mixture composed of 0.01 mole of L-glutamic acid and 0.02 mole of glycine was ground together in a mortar. This mixture was heated and melted in an open flask at 175–190 °C for approximately 20 min in a microwave reactor. In the experiments performed in the presence of mineral, 0.100 g of aluminum oxide was used. When the reaction was completed a brown liquid that solidified upon cooling was obtained. For vibrational measurements the solid residue was washed with 10 mL of deionized water and was allowed to settle down during 24 h. The solid obtained after 24 h was centrifuged, dried at 50 °C and weighted for yield calculation.

2.3. Infrared and Raman spectra

Infrared (IR) spectra were measured on a Fourier Transform Infrared (FT-IR) Perkin Elmer Spectrum RX spectrometer provided with a DTGS (Deuterated TriGlycerine Sulfate) detector. The spectral resolution was 4 cm^{-1} and 16 scans were obtained on each sample. KBr pellets were prepared by mixing 1 mg of sample and 200 mg of KBr.

The Raman spectra were recorded with a Renishaw Raman Microscope System RM2000 equipped with a diode laser providing a 634 nm line, a Leica microscope, an electrically cooled CCD (Charge Coupled Device) detector and a notch filter to eliminate the elastic scattering. The spectra were obtained by using a 100× objective. The laser power output was 2.0 mW and the spectral resolution was 2 cm^{-1}.

2.4. Scanning Electron Microscopy and Energy Dispersive X-ray analysis (SEM–EDX)

The samples were homogenized by grinding and the powder samples were fixed on an adhesive carbon band. A Scanning Electron Microscope (SEM) JEOL JSM6360 LV coupled to an Energy Dispersive X-ray (EDX) spectrometer Inca Oxford was used for the analysis. SEM photographs were taken at 30×, 100× and 500× and on each of them a chemical mapping analysis was made with the following color reference: aluminum in red, carbon in green and oxygen in blue.

2.5. Sodium dodecyl sulfate polyacrylamide gel electrophoresis analysis (SDS–PAGE)

0.5 mg of the samples were dissolved in 1 mL of 0.1 M borate buffer pH 9. The insoluble fraction was separated by microcentrifugation 5 min at 14,000 rpm. Then, 3 mg of fluorescamine were added. 15 μL of each sample were mixed with loading buffer solution and load onto the gel and electrophoresed according to Lagos et al. (2001). The polyacrylamide gel (PAG) was prepared as a discontinuous gradient of acrylamide concentration: 3, 10 and 16%. A peptide molecular weight marker from Sigma® (2–17 kDa) was used.

2.6. Theory/calculation

Theoretical infrared and Raman spectra were calculated from Density Functional Theory (DFT). The structure and vibrational frequencies of the Gly-Glu dipeptide were determined using the Gaussian 03W program package (Frisch et al., 2003). The Becke's three-parameter hybrid method using the Lee–Yang–Parr correlation functional (B3LYP) together with the 6-31G** basis set were used in the geometry optimization and calculations of the normal modes. At the optimized structure of the dipeptide, no imaginary frequencies were obtained, providing that a local minimum on the potential energy surface was found.

3. Results

3.1. Vibrational assignments

The bands assignment were performed on the basis of published data of related molecules (Baran and Ratajczak, 2005; Dhamelincourt and Ramirez, 1991; Fischer et al., 2005; Kumar et al., 2005; Peica et al., 2007; Vijay and Sathyanarayana, 1992) and general characteristic group frequencies (Barth, 2007; Colthup et al., 1990; Pearson and Slifkin, 1972; Socrates, 2000). Theoretical infrared and Raman frequencies are in good agreement with the experimental corresponding data. Moreover, the results allowed completing the experimental band assignment and distinguishing overlapped components in broad bands.

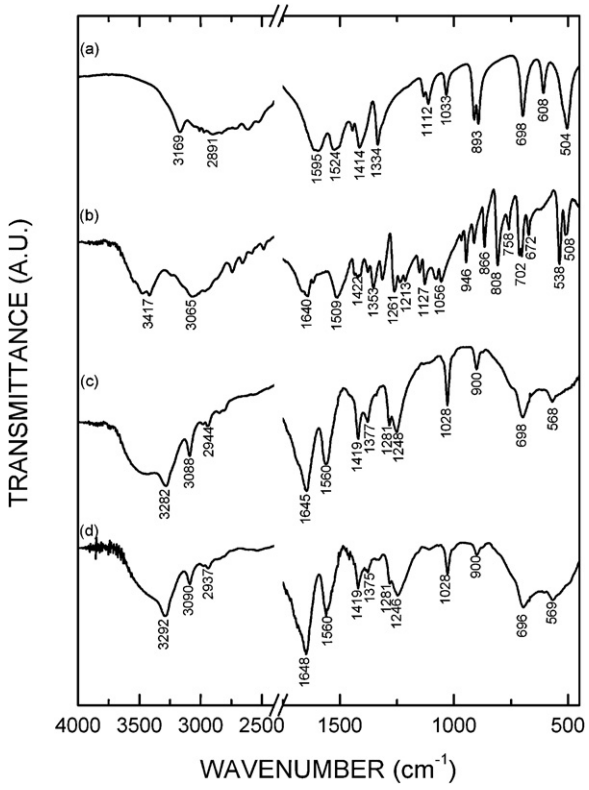

Fig. 1. Infrared experimental spectra in KBr pellet obtained for (a) glycine (Gly), (b) glutamic acid (Glu), (c) polymer obtained by thermal synthesis in the absence of Al_2O_3, and (d) polymer obtained by thermal synthesis in the presence of Al_2O_3.

3.1.1. Glycine (Gly)

The infrared and Raman spectra of glycine (Gly) in solid are displayed in Figs. 1a and 2a, respectively. All vibrational modes are both infrared and Raman active. Table 1 lists the observed infrared and Raman frequencies and the proposed band assignments.

The Raman spectrum showed the characteristic $\nu_{as}(NH_2)$ mode at 3143 cm^{-1}, and aliphatic vibrations $\nu_{as}(CH_2)$ at 3007 cm^{-1} and $\nu_s(CH_2)$ at 2965 cm^{-1}. Three weak bands observed at 1667, 1629 cm^{-1} and 1568 cm^{-1} in the Raman spectra were assigned to $\nu_s(C{=}O)$, $\delta_{as}(NH_2)$ and the asymmetric stretching of the COO moiety of the COOH group $\nu_{as}(COOH)$, respectively. Bands at about 1514 and 1454 cm^{-1} were assigned to bending (scissoring) of the NH_2 and CH_2 groups, respectively. The band at 1410 cm^{-1} was ascribed to the $\nu_s(COOH)$ mode. The intense band observed at 1322 cm^{-1} was assigned to a CH deformation.

The two weak bands in the Raman spectrum at 1138 and 1104 cm^{-1} were assigned to rocking of the NH_2 group (Fischer et al., 2005). A sharp band with medium intensity observed at 1033 cm^{-1} in the IR spectrum and at 1034 cm^{-1} in the Raman spectrum was assigned to a coupled vibration ν(C–N + C–C) (Kumar et al., 2005). The region between 1000 and 350 cm^{-1} showed a medium intensity band in the infrared spectrum at 911 cm^{-1}, which was assigned to CH_2 bending, a coupled vibration at 893 cm^{-1} for the NH_2 twist plus a CH_2 twist, and NH_2 bending at 698 cm^{-1} (Kumar et al., 2005). Also, there were two bands in the spectrum located at 608 and 504 cm^{-1} both related to the carboxylic acid fragment (Kumar et

Table 1
Experimental data for the vibrational spectra of glycine (Gly) and glutamic acid (Glu).

Gly Wavenumber (cm^{-1})[b]		Glu Wavenumber (cm^{-1})		Vibrational assignment[a]
IR	Raman	IR	Raman	
		3417 s, br		ν(OH)
3169 s		3065 s, br		$\nu_{as}(NH_2)$
	3143 m		3015 vw	$\nu_{as}(NH_2)$
			2990 w	¿ν(NH)?
3011 s	3007 s		2967 w	$\nu_{as}(CH_2)$
2971 s	2977 sh	2962 sh	2961 sh	ν(CH)
	2965 vs		2931 w	$\nu_s(CH_2)$
2891 br				$\nu_s(CH_2)$
2615 m		2659 m		$\nu_s(NH_2)$
2125 w		2079 w		$\nu_s(NH_2)$
n.d.	1667 w	1665 sh	n.d.	ν_s(C=O)
	1629 vw		1653 w	$\delta_{as}(NH_2)$
1613 sh		1640 s		$\delta_{as}(NH_2)$
1595 s		1617 m		ν_{as}(COOH)
	1568 vw		n.d.	ν_{as}(COOH)
1524 s		1509 s	n.d.	$\delta_s(NH_2)$
	1514 w			$\delta_s(NH_2)$
1445 m	1454 w	1434 sh	1437 w	$\delta(CH_2)$
1414 s	1410 w	1422 m		ν_s(COOH)
			1405 m	ν_s(COOH)
		1377 w		$\omega(CH_2)$
1334 s		1353 m		δ(CH)
	1322 m		1346 m	δ(CH)
		1314 m	1307 m	δ(OH)
		1261 s	1253 vw	δ(CH)
		1234 m		$\tau(CH_2)$
		1213 m		$\tau(CH_2)$
1132 w	1138 w	1151 m	1148 w	$\rho(NH_2)$
1112 m	1104 vw	1127 s	1127 w	$\rho(NH_2)$
		1078 m	1083 w	ν(C–O)
1033 m	1034 w			ν(C–N) + ν(C–C)
		1056 s	1057 w	ν(C–N)
		968 w	966 m	ν(C–C)
		946 m	939 w	γ(OH)
		913 w	916 m	ν(C–C)
911 m				$\delta(CH_2)$
893 m	890 w			$\tau(NH_2) + \tau(CH_2)$
		866 m	863 s	δ(COOH)
		808 s	798 m	ν(C–C)
		758 w	758 m	$\rho(CH_2)$
		712 m	n.d.	$\rho(CH_2)$
		702 m	704 m	δ(COOH)
698 m	697 vw			$\delta(NH_2)$
		672 m	n.d.	δ(COOH)
608 m	601 vw			δ(COOH) + δ(NCCO)
		538 s	534 m	γ(OCC)
		508 m	499 m	$\rho(COOH) + \tau(NH_2)$
504 s	n.d.			$\delta(COOH) + \delta(CH_2)$
		n.d.	459 w	$\tau(NH_2)$
n.i.	357 vw	n.i.	384 m	δ(skel)
		n.i.	253 w	δ(skel)

[a] ν = stretching; as = antisymmetric; s = symmetric; δ = bending; ρ = rocking; ω = wagging; τ = torsion; γ = out of the plane bending.
[b] vw = very weak; w = weak, m = medium, br = broad, sh = shoulder, s = strong, vs = very strong, n.d. = non-detected, n.i. = non-investigated.

al., 2005). Finally, a very weak band was observed at 357 cm^{-1} in the Raman spectrum which was tentatively assigned to skeletal vibrations.

3.1.2. Glutamic acid (Glu)

The infrared and Raman spectra of L-glutamic acid (Glu) in the solid state are displayed in Figs. 1b and 2b, respectively. Table 1 lists the observed infrared and Raman frequencies and the proposed band assignments for glutamic acid. In the infrared spectrum of glutamic acid, a broad characteristic band with strong intensity observed at 3417 cm^{-1} was attributed to ν(OH). The broad band at 3064 cm^{-1} was assigned to $\nu_{as}(NH_2)$ and the band at 2962 cm^{-1} was assigned to the ν(CH) vibration. The vibration observed in the Raman spectrum at 2990 cm^{-1} was tentatively assigned to ν(NH), and absorptions at 2967 and 2931 cm^{-1} were attributed to $\nu_a(CH_2)$ and $\nu_s(CH_2)$, respectively. The region between 1800–1500 cm^{-1} showed a group of vibrations close to each other; a shoulder at 1665 cm^{-1} with medium intensity in the IR spectrum was assigned to ν_s(C=O) stretching, along with a second absorption at 1640 cm^{-1} of strong intensity in the IR and weak intensity in the Raman spectra that was attributed to the $\delta_{as}(NH_2)$ mode. The last band of this group located around 1617 cm^{-1} in the infrared spectrum, was assigned to ν_a(COOH). In the region between 1500 and 1100 cm^{-1} was observed a set of bands; the vibration at 1509 cm^{-1}, which was attributed to $\delta_s(NH_2)$, an absorption at 1434 cm^{-1} corresponding to the $\delta(CH_2)$ mode and another at 1422 cm^{-1} in the IR and at 1405 cm^{-1} in the Raman spectra of medium to strong intensity, were assigned to the ν_s(COOH) vibration. The band at 1377 cm^{-1} was assigned to CH_2 wagging; as well as absorptions at 1353 and 1261 cm^{-1} which were ascribed to δ(CH). Absorption at 1314 cm^{-1}

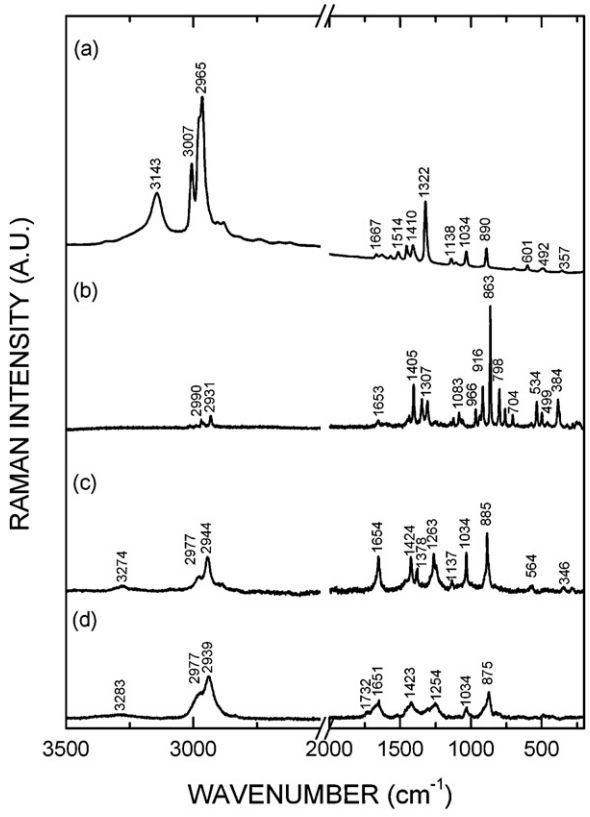

Fig. 2. Raman experimental spectra obtained for (a) glycine (Gly), (b) glutamic acid (Glu), (c) polymer obtained by thermal synthesis in the absence of Al_2O_3, and (d) polymer obtained by thermal synthesis in the presence of Al_2O_3.

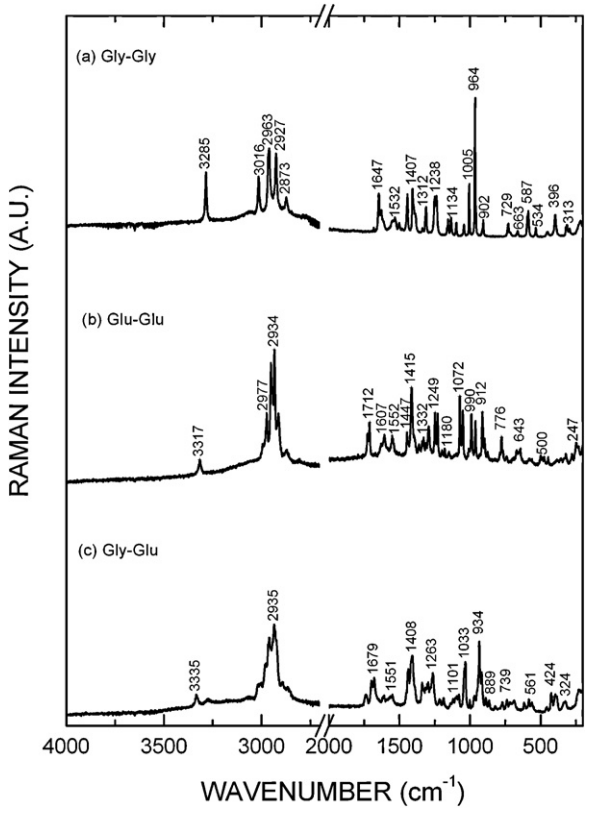

Fig. 3. Raman experimental spectra obtained for (a) glycylglycine (Gly-Gly), (b) glutamyl-glutamic acid (Glu-Glu) and (c) N-glycylglutamic acid (Gly-Glu).

was assigned to δ(OH), while absorptions at 1234 and 1213 cm^{-1} were assigned to CH_2 torsional bending. Finally, absorptions at 1151 and 1127 cm^{-1} were assigned to rocking of the NH_2 group (Dhamelincourt and Ramirez, 1991).

The band located at 1084 cm^{-1} in the Raman spectrum and at 1078 cm^{-1} in the infrared spectrum correspond to the ν(C–O) vibration, while the band observed at 1057 cm^{-1} in the Raman spectrum and 1056 cm^{-1} in the infrared spectrum was attributed to ν(C–N). In the region between 1000 and 800 cm^{-1}, three bands that correspond to carbon skeletal CC stretching vibrations were observed at 968, 913 and 808 cm^{-1} (Dhamelincourt and Ramirez, 1991). The bands observed at 758 and 712 cm^{-1} in the IR spectrum were assigned to CH_2 rocking. The bands observed at 702 and 672 cm^{-1} were assigned to bending of the COOH group (Dhamelincourt and Ramirez, 1991; Peica et al., 2007). The region of the spectrum under 600 cm^{-1} was difficult to interpret because of the appearance of bending and torsional vibrations of the molecular structure, as well as other coupled vibrations such as the rocking of the COOH group and torsional vibrations of the NH_2 group observed at 508 cm^{-1} in the infrared spectrum and 499 cm^{-1} in the Raman spectrum (Peica et al., 2007). All of these modes were usually overlapping and the assignments made in this region are therefore tentative.

3.1.3. Polymeric (Gly-Glu-(Gly-Glu)$_n$)

The infrared and Raman spectra of the product obtained from the thermal synthesis in the absence (Figs. 1c and 2c) and in the presence of aluminum oxide (Figs. 1d and 2d), were very similar. These clearly showed the appearance of a strong intensity band at 1647 cm^{-1} in the infrared spectrum and at 1654 cm^{-1} in the Raman spectrum, which was assigned to amide I and arises mainly from the C=O stretching vibration, with minor contributions from out of the phase CN stretching vibrations, CCN deformation and NH in-plane bending. This absorption overlapped with the band at 1560 cm^{-1} in the infrared spectrum, which corresponded to the amide II mode (δ(NH) + ν(CN)). In this sense, the bands located at 1281 cm^{-1} in the infrared spectrum and 1263 cm^{-1} in the Raman spectrum correspond to the amide III mode which is the in-phase combination of NH bending and CN stretching vibrations, with small contributions from the δCO and νCC modes. All three of these bands appeared at characteristic wavenumbers usually assigned to a polypeptide with the α form (Socrates, 2000). However, an expected strong intensity band associated to the skeletal mode in the 900–960 cm^{-1} region in the Raman spectra is not observed, which suggests that the polypeptide obtained has a random coil structure (Carey and Salares, 1980).

Additionally, the absorptions located at 3286 cm^{-1} and 3088 cm^{-1} were assigned to the ν_a(N–H) and ν_s(N–H) modes, respectively. Table 2 lists the observed infrared and Raman frequencies and the proposed band assignments for the polymers obtained from the synthesis in the absence and presence of Al_2O_3.

An IR and Raman characterization of glycylglycine (Gly-Gly), glutamyl-glutamic acid (Glu-Glu) and N-glycylglutamic acid (Gly-Glu) dipeptides reagents p.a. allowed the acquisition of more information about the polypeptide obtained. Peptides generally display the same type of vibrational spectra as their component amino acids combined with other bands attributed to the characteristic bands for the peptide bond. Based on previously reported data for glycine (Baran and Ratajczak, 2005; Fischer et al., 2005; Kumar et al., 2005; Vijay and Sathyanarayana, 1992), glutamic acid (Dhamelincourt and Ramirez, 1991; Peica et al., 2007) and glycyl-glycine dipeptide (Gly-Gly) (Fischer et al., 2005; Zhao et al., 2008), and the present calculations made for the Gly-Glu dipeptide, the assignments in Table 3 for the dipeptides were proposed. The Raman spectra obtained for the dipeptides p.a. are shown in Fig. 3.

Table 2
Experimental data for the vibrational spectra for the synthesized polypeptide.

Polymer Wavenumber (cm^{-1})[b]		Polymer/Al_2O_3 Wavenumber (cm^{-1})		Vibrational assignment[a]	Comments
IR	Raman	IR	Raman		
3282 s	3274 w	3292 s	3283 vw	$\nu_a(NH_2)$	Intensity increases with molecular weight
3088 m	n.d.	3090 m	n.d.	$\nu_s(NH_2)$	Intensity increases with molecular weight
2971 w	2977 m	2978 vw	2977 m	$\nu_a(CH_2)$	
2944 w	2944 s	2937 w	2939 s	$\nu_S(CH_2)$	
n.d.	n.d.	n.d.	1732 w	ν(C=O)	COOH fragment R of GLU
1645 s	1654 m	1648 s	1651 m	ν(C=O) + ν(CN) + δ(NH)	Amide I (α form)
1560 s	n.d.	1560 s	n.d.	δ(NH) + ν(CN)	Amide II (α form)
1419 m	1424 s	1419 m	1423 m	ν_s(COOH)	
1377 m	1378 m	1375 m	1254 m,br	$\omega(CH_2)$	
1281 m	1263 s	1281 m	1254 m,br	ν(CN) + δ(NH) + ν(CO) + δ(O=CN)	Amide III (α form)
1248 m	1244 m	1246 m	1254 m,br	$\rho(NH_2)$	
n.d.	1137 w	n.d.	n.d.	$\rho(NH_2)$	
1028 m	1034 s	1028 m	1034 m	ν(C–N) + ν(C–C)	
900 m	885 s	900 w	875 m	ν_s(CNC)	
698 m	n.d.	696 m	n.d.	δ(NC=O)	Amide IV
568 w	564 w	569 w	n.d.	δ(C=O)	Amide VI
n.i.	346 vw	n.i.	n.d.	δ(skel)	
n.i.	286 vw	n.i.	n.d.	δ(skel)	

[a] ν = stretching; as = antisymetric; s = symetric; δ = bending; ρ = rocking; ω = wagging; τ = torsion; γ = out of the plane bending.
[b] vw = very weak; w = weak, m = medium, br = broad, sh = shoulder, s = strong, vs = very strong, n.d. = non-detected, n.i. = non-investigated.

The band centered at 1034 cm^{-1} in the Raman spectrum of glycine was observed in the Gly-Glu dipeptide at 1033 cm^{-1}. In the polypeptide, it was observed at 1028 cm^{-1} in the infrared spectrum and at 1034 cm^{-1} in the Raman spectrum and corresponded to ν(CN) coupled to ν(CC) of the glycine fragment (Kumar et al., 2005). On the other hand, the band centered at 1056 cm^{-1} in the infrared spectra of glutamic acid attributed to ν(C–N) (Dhamelincourt and Ramirez, 1991) disappears in the polypeptide spectra indicating that the predominant bonding in the peptide bond is Gly-Glu. Theoretical infrared and Raman frequencies are in good agreement with the experimental corresponding data. Then, it is possible to argue that the proposed structure for the Gly-Glu-(Gly-Glu)$_n$ experimental sequence is adequate (see Fig. 4).

3.2. Scanning Electron Microscopy–Energy Dispersive X-ray analysis

According to the SEM images (Fig. 5a) the morphology of the aluminum oxide crystal used for the synthesis (light grey crystals) did not change under the thermal treatment. The SEM–EDX analysis of the sample of Gly-Glu-(Gly-Glu)$_n$ polymer on Al_2O_3 is shown in Fig. 5b. As can be seen in the microphotography obtained at 500×, only Al, C, N and O were detected in the sample and according to the color assignment (red for aluminum, green for carbon and blue for oxygen), all of the particles of aluminum oxide (pink color) were surrounded by polymer (green–blue color). As can be seen in the individual elemental mapping (Fig. 5c), the green–blue zones had nitrogen signals as well, which corresponds to the elemental composition of the polymer. This approach shows the growth of the polymer (green–blue color) on an aluminum oxide particle surface (pink color).

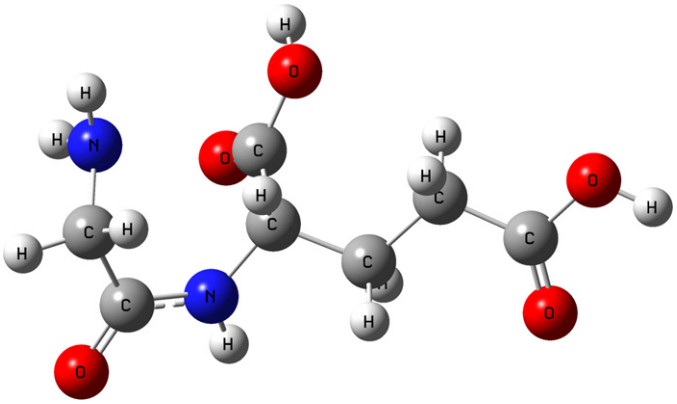

Fig. 4. Final geometry of the Gly-Glu dipeptide.

3.3. Sodium dodecyl sulfate polyacrylamide gel electrophoresis (SDS–PAGE)

In Fig. 6, the results obtained by SDS–PAGE are shown. The polypeptide obtained in the absence of Al_2O_3, shows two main signals, the first between 10.8 and 4.4 kDa and the second is below 1 kDa. The sample obtained in the presence of aluminum oxide shows a polydispersive population of peptides from 9.4 kDa until less than 1 kDa, with a larger population in the area of low molecular weight polypeptides. The sample obtained in the absence of Al_2O_3 should contain around 60 amino acid units, while the polypeptide obtained in the presence of Al_2O_3 should have between 10 and 90 amino acid units.

4. Discussion

This thermal polymerization was performed in the molten state. In this case, the reaction products were mainly determined based on the temperature of the melting process. In the glycine and glutamic acid condensation reactions has been reported that the order of the amino acids residues could not be completely random due to pyroglutamic acid formation and high reactivity of glycine under thermal conditions (Mandal and Balaram, 2007; Panday et al., 2009; Righetti and Tamba, 1982; Soloshonok et al., 2005).

There was no difference between the infrared and Raman spectra profiles of the obtained products from the thermal synthesis in the presence and absence of mineral surfaces used in this study. The spectra coincide with the preferential Gly-Glu-(Gly-Glu)$_n$ polymer sequence with random coil. The theoretical spectral data support the experimental proposed Gly-Glu-(Gly-Glu)$_n$ main sequence for the polymer. The preferential sequence in peptides obtained by thermal condensation has been reported earlier (Fox et al., 1977; Hartmann et al., 1981), as well as the formation of linear polypeptides (Fouche and Rohlfing, 1976; Harada and Fox, 1958; Rohlfing

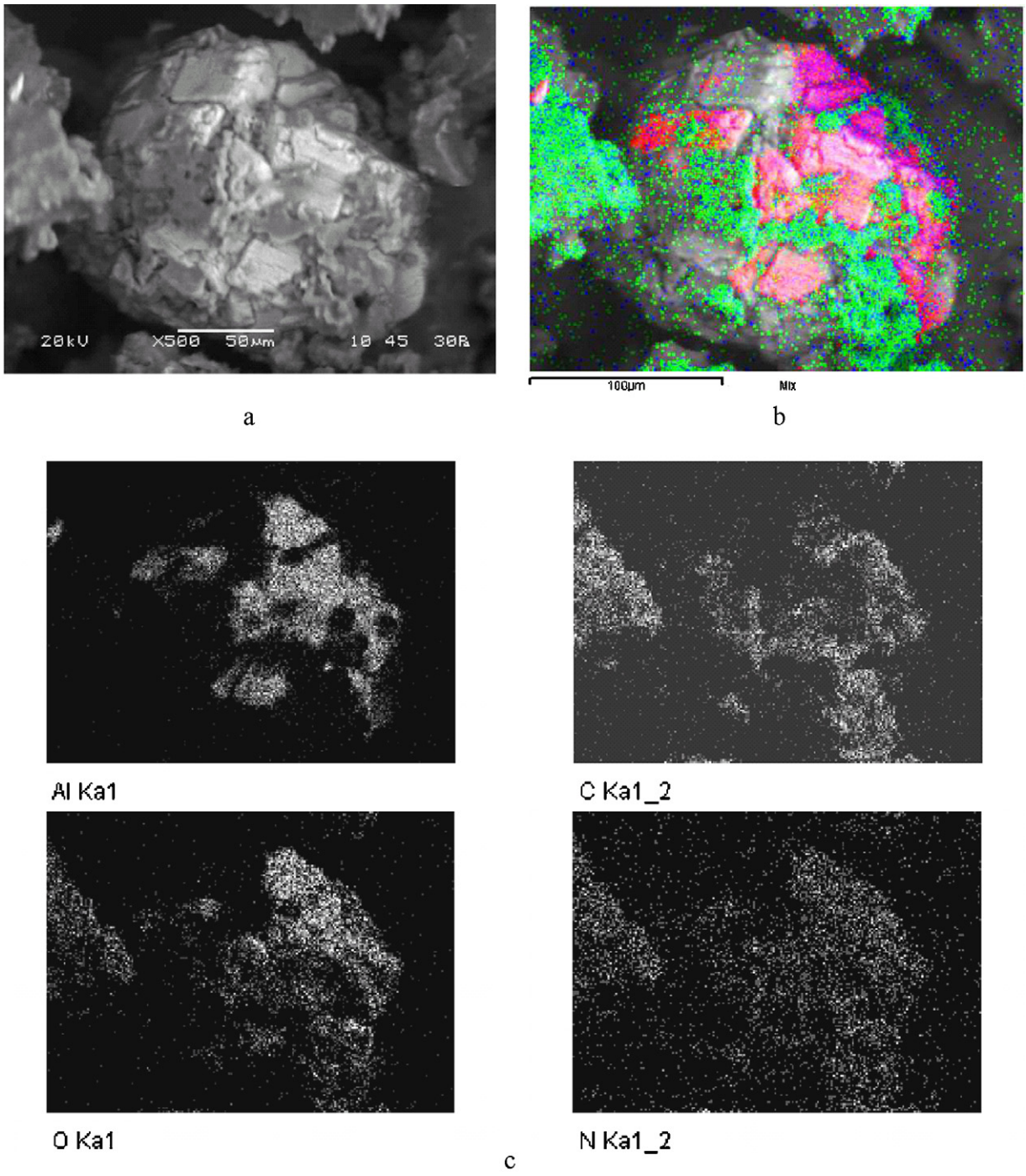

Fig. 5. SEM–EDX results for the approach on the Gly-Glu polymer on aluminum oxide. (a) Scanning electron image (500×) of Gly-Glu polymer on aluminum oxide (white crystals) (b) Elemental mapping analysis made at 500× on Gly-Glu polymer on aluminum oxide. (: Al; : C and : O) (c) Individual elemental mapping results of Gly-Glu polymer on aluminum oxide obtained at 500×.

and MacAlhaney, 1976). The bandwidth spectral increasing of the synthetic polypeptide and a positive Biuret response (data not shown) are evidence of a polymeric structure.

The mechanism of this preferential Gly-Glu sequence could be through the formation of diketopiperazin (DKP) rings between glycine and glutamic acid, indicating that the formation of the peptide bonds proceeds through the nucleophilic attack of an amino group of the amino acids on the DKP accompanied by the ring-opening (Kawamura et al., 2009; Mosqueira et al., 2008; Parrish and Mathias, 2002). For these reason there was not observed bands associated to DKP ring breathing vibrations that usually appear at 914 and 809 cm^{-1} in the vibrational spectra of the product obtained (Cheam and Krimm, 1984a,b). In this context, the formation of lineal peptides instead of diketopiperazines when two or more aminoacids are heated has been reported (Fouche and Rohlfing, 1976; Guo et al., 2006; Harada and Fox, 1958; Hartmann et al., 1981; Meng et al., 2004; Rohlfing and MacAlhaney, 1976).

SEM–EDX characterization of the solid phase involved in the thermal synthesis showed that the aluminum oxide participate as a site for nucleation and growth of the polymer explaining the increase of 25% on gravimetric yield in the presence of oxide (data not shown). This result suggests that, during the thermal treatment,

Table 3
Experimental infrared and Raman frequencies for glycylglycine (Gly-Gly) and glutamyl-glutamic acid (Glu-Glu). Experimental Infrared and Raman and Raman calculated data for N-glycylglutamic acid (Gly-Glu).

Gly-Gly Wavenumber (cm^{-1})[b]		Glu-Glu Wavenumber (cm^{-1})		Gly-Glu Wavenumber (cm^{-1})			Vibrational assignment[a]	Comments/References
IR	Raman	IR	Raman	IR	Raman	Calculated		
3286 br	3285 s	3316 s	3317 m	3334 s	3335 m	3420	ν(NH)	Socrates (2000)
3065 sh	n.d.	3100 s,br	–	3074 s,br	–	3032	ν(NH)	Overtone of Amide II
n.d.	3016 m				3013 w	3011	$\nu_a(CH_2)$	
2970 m	2963 s		2977 m		2961 s	2967	$\nu_s(CH_2)$	
			2951 s				ν(CH)	
2929 sh	2927 s		2934 s		2935 s	2952	$\nu(CH_2)$	
2880 sh	2873 m		2913 m		2922 sh	2923	$\nu(CH_2)$	
		1730 s	1726 w	1734 m	1739 w	1769	ν(C=O)	Barth (2007)
1676m,br	1682 vw	1716 s	1712 m	1700 m	1697 m	1710	ν_a(COOH)	
1654m,br	1647 m	1630 sh	1631 sh	1684 m	1679 m	1652	ν(C=O) + ν(CN) + δ(NH)	Amide I
1629m,br	1629 w	1610 s	1607 w	1613 sh	1607 w	–	$\delta_a(NH_2)$	
1602m,br	n.d.	1586 s	n.d.	1584 sh	n.d.	–	ν_a(COOH)	
1558 w	1551 sh	1553 m	1552 w	1556 s	1551 w	1579	δ(NH) + ν(CN)	Amide II
–	1532 m						$\delta(NH_2)$	
1481 m	1479 vw			1453 w	–	1454	$\delta(CH_2)$	Fischer et al. (2005)
1442 m	1444 m	1438 sh	1447 m	1436 w	1437 m	1426	$\delta(CH_2)$	
1407s	1407 m	1415 m	1415 s	1405 m	1408 m	1410	$\nu\nu_s$(COOH)	Dhamelincourt and Ramirez (1991) and Fischer et al. (2005)
		1395 m	1396 sh				$\omega(CH_2)$	Dhamelincourt and Ramirez (1991)
		1362 w					¿δ(CH)?	
1336 m	1338 w	n.d.	1332 w	1334 w	1340 w	1362	δ(CH)	Dhamelincourt and Ramirez (1991) and Fischer et al. (2005)
1310 m	1312 m						$\delta(CH_2)$	Fischer et al. (2005)
		1313 m	1312 w	–	1316 w	1315	δ(OH)	Dhamelincourt and Ramirez (1991)
		1290 m	1293 m	1303 m	1297 w	1301	δ(COH)	Barth (2007)
		1278 m	n.d.				$\omega(CH_2)$	Peica et al. (2007)
1253 m	1250 m	1249 m	1249 m	1265 m	1263 m	1279	ν(CN) + δ(NH) + ν(CO) + δ(O=CN)	Amide III
1231 w	1238 m		1231 m				$\delta(CH_2)/\omega(NH_2)$	Fischer et al. (2005)/Zhao et al. (2008)
		1238 m	n.d.	1234 w	n.d.	1242	$\tau(CH_2)$	Dhamelincourt and Ramirez (1991)
		1197 m	1199 vw	1216 sh	1217 w	1206	$\tau(CH_2)$	Barth (2007)
		1182 m	1180 vw	1189 m	1189 w	1184	ν(CO)	Barth (2007)
1158 m	1155 m						δ(NH)	Fischer et al. (2005) and Zhao et al. (2008)
1134 m	1134 m	1152 w	1149 w	–	–	–	$\rho(NH_2)$	Dhamelincourt and Ramirez (1991) and Fischer et al. (2005)
1086 s	1089 m	1097 m	1096 w	1105 w	1101 w	1094	$\delta(NH_2)$	Fischer et al. (2005)
		1073 w	1072 m	1080 w	1081 w	1052	ν(C–O)	Dhamelincourt and Ramirez (1991)
1048 s	1043 m	1053 w	1051 m	1033 w	1033 m	1024	ν(C–N) + ν(C–C)	
1002 m	1005 m						$\delta(CH_2)/\nu(NH_2)$	Fischer et al. (2005)/Zhao et al. (2008)
		1005 w	1007 vw	n.d.	1001 w	1001	γ(CH)	
966 m	964 s						$\omega(CH_2)$	Zhao et al. (2008)
		990 w	990 m				¿?	
				966 w	969 w	972	ν(CC)	Dhamelincourt and Ramirez (1991)
		n.d.	961 m	933 w	934 s	–	γ(OH)	Dhamelincourt and Ramirez (1991)
918 m	n.d.						γ(CH)/ν(CN)	Zhao et al. (2008)/Fischer et al. (2005)
		914 w	912 m	913 m	918 m	905	ν(CC)	Dhamelincourt and Ramirez (1991)
900 m	902 m						$\delta(CH_2)$	Fischer et al. (2005)
880 m	n.d.						$\tau(NH_2) + \tau(CH_2)$	Fischer et al. (2005)
		884 w	889 m	892 w	889 w	884	δ(COOH)	Dhamelincourt and Ramirez (1991)
		830 m	n.d.	824 w	823 vw	826	δ(CO) + δ(NH)	Peica et al. (2007)
		790 m	n.d.	792 vw	n.d.	797	$\delta(NH_2)$	
		n.d.	776 w				¿$\delta(NH_2)$?	Dhamelincourt and Ramirez (1991)
731 m	729 w						$\omega(NH_2)$	Zhao et al. (2008)
		744 m	n.d.	742 m	739 w	770	δ(COOH)/$\rho(CH_2)$	Peica et al. (2007)/Dhamelincourt and Ramirez (1991)
710 m	717 sh						$\omega(CH_2)$	Zhao et al. (2008)
		705 m	n.d.	698 w	696 w	724	$\rho(CH_2)$	Dhamelincourt and Ramirez (1991)
663 m	663 w						ν(NH)	Zhao et al. (2008)
		671 m	668 w	668 w	n.d.	650	δ(COOH)	Dhamelincourt and Ramirez (1991)
		646 m	643 w	622 w	618 w	621	¿?	
591 m	587 m	583 w	579 vw	584 m	583 w	604	ν(NH)/δ(O=C–N)	Zhao et al. (2008)/Socrates (2000)
				560 w	561 w	553	δ (C=O)	Amide VI/Socrates (2000)
531 m	534 w						ν_a(NCC)	Zhao et al. (2008)
		501 vw	500 vw				δ (COOH)	Dhamelincourt and Ramirez (1991)
		479 w	474 vw				$\tau(NH_2)$	Peica et al. (2007)
		451 w	447 vw	458 w	456 vw	454	$\tau(NH_2)$	Dhamelincourt and Ramirez (1991)
437 sh	440 vw						τ(CC=O)	Zhao et al. (2008)
				n.d.	424 w	417	δ(OH, CH)	Peica et al. (2007)
402 m	396 m						¿?	
				405 m	400 w	387	δ(skel)	Dhamelincourt and Ramirez (1991)
n.i.	313 w			n.i.	324 w	329	¿δ(skel)?	
n.i.	293 vw	n.i.	247 w				δ(skel)	Dhamelincourt and Ramirez (1991)
n.i.	215 w			n.i.	229 m	241	δ(skel)	Dhamelincourt and Ramirez (1991)

[a] ν = stretching; as = antisymmetric; s = symmetric; δ = bending; ρ= rocking; ω = wagging; τ = torsion; γ = out of the plane bending.
[b] vw = very weak; w = weak, m = medium, br = broad, sh = shoulder, s = strong, vs = very strong, n.d. = non-detected, n.i. = non-investigated.

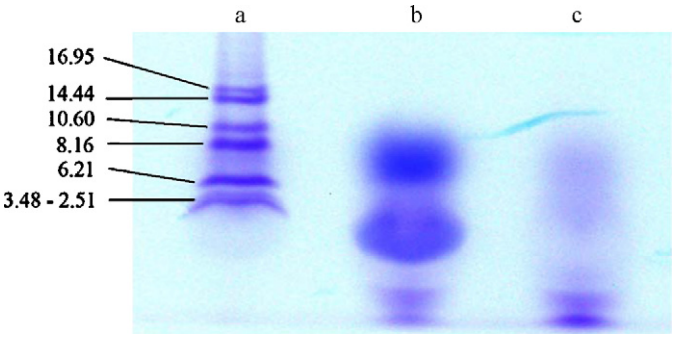

Fig. 6. SDS–PAGE results for (a) molecular weight markers, (b) Gly-Glu polymer obtained by thermal synthesis in the absence of aluminum oxide, and (c) polymer obtained by thermal synthesis in the presence of Al_2O_3.

aluminum oxide act as a nucleation site for the Gly-Glu-(Gly-Glu)$_n$ polymer. Moreover, the SDS–PAGE results showed an increase of the peptide chain length in the absence of aluminum oxide; allowing for the postulation that a greater number of polymer chains of shorter length were formed in the presence of Al_2O_3 compared to the test conducted in the absence of aluminum oxide. In this sense, it could be possible to argue that the active Lewis sites, obtained by alumina heating could be used by any negative moiety of the amino acids Gly or Glu, thus controlling the length of the polypeptidic chain, this is being matter of further studies. However, some authors have found that pure alumina can be involved in the processes of chain elongation and stabilization in SIPF reactions (Rode et al., 1999).

First proteins involved in the formation of living cells could have been condensed phases of these polypeptides, which could have been formed from amino acids, at the surfaces of minerals similar to aluminum oxide (Bujdák and Rode, 2001, 2002). Given the variety of amino acids and monomers emerged during chemical evolution, the complexity of these polymers could be considerable (Bujdák and Rode, 2002).

5. Conclusions

There was no difference between the IR and Raman spectral profiles of the obtained product from the thermal synthesis in the presence and absence of mineral surfaces used in this study. The observed spectral bandwidth increasing in the synthetic polypeptide is in agreement with a polymeric structure. The theoretical spectral data support the experimental proposed Gly-Glu-(Gly-Glu)$_n$ main sequence for the polymer. SEM–EDX characterization of the solid phase involved in the thermal synthesis showed that the aluminum oxide participate as a site for nucleation and growth of the polymer explaining the increase of 25% on gravimetric yield in the presence of oxide. In this sense, SDS–PAGE data showed oligopeptides in the presence of aluminum oxide, allowing for the postulation that a greater number of polymer chains of shorter length were formed in the presence of Al_2O_3 compared to the test conducted in the absence of aluminum oxide.

Acknowledgement

This research has been financially supported by project 1085124 from Fondecyt.

References

Banerjee, D.P.K., Misselt, K.A., Su, K.Y.L., Ashok, N.M., Smith, P.S., 2007. Spitzer observations of V4332 Sagittarii: detection of alumina dust. The Astrophysical Journal 666, L25–L28.

Baran, J., Ratajczak, H., 2005. Polarised IR and Raman spectra of the γ-glycine single crystal. Spectrochimica Acta Part A 61, 1611–1626.

Barth, A., 2007. Infrared spectroscopy of proteins. Biochimica et Biophysica Acta 1767, 1073–1101.

Bujdák, J., Rode, B.M., 2001. Activated alumina as an energy source for peptide bond formation: consequences for mineral-mediated prebiotic processes. Amino Acids 21, 281–291.

Bujdák, J., Rode, B.M., 2002. Preferential amino acid sequences in alumina-catalyzed peptide bond formation. Journal of Inorganic Biochemistry 90, 1–7.

Carey, P.R., Salares, V.R., 1980. Raman and resonance Raman studies of biological systems. In: Clark, R.J.H., Hester, R.E. (Eds.), Advances in Infrared and Raman Spectroscopy. Heyden & Sons Ltd., London, pp. 1–45.

Colthup, N.B., Daly, L.H., Wiberley, S.E., 1990. Introduction to Infrared and Raman Spectroscopy. Academic Press, London.

Cheam, T.C., Krimm, S., 1984a. Vibrational analysis of crystalline diketopiperazine – I. Raman and IR spectra. Spectrochimica Acta Part A: Molecular Spectroscopy 40, 481–501.

Cheam, T.C., Krimm, S., 1984b. Vibrational analysis of crystalline diketopiperazine – II. Normal mode calculations. Spectrochimica Acta Part A: Molecular Spectroscopy 40, 503–517.

Dhamelincourt, P., Ramirez, F.J., 1991. Polarized micro-Raman and Fourier transform infrared spectra of L-glutamic acid. Journal of Raman Spectroscopy 22, 577–582.

Fischer, G., Cao, X., Cox, N., Francis, M., 2005. The FT-IR spectra of glycine and glycylglycine zwitterions isolated in alkali halide matrices. Chemical Physics 313, 39–49.

Fouche Jr., C.E., Rohlfing, D.L., 1976. Thermal polymerization of amino acids under various atmosphere or at low pressures. Biosystems 8, 57–65.

Fox, S.W., Melius, P., Nakashima, T., 1977. N-terminal pyroglutamyl residues in proteins and thermal peptides. In: Matsubara, H., Yamanaka, T. (Eds.), Symposium on Evolution of Proteins. Japan Scientific Societies Press, Osaka-Kobe, pp. 111–120.

Frisch, M.J., Trucks, G.W., Schlegel, H.B., Scuseria, G.E., Robb, M.A., Cheeseman, J.R., Montgomery Jr., J.A., Vreven, T., Kudin, K.N., Burant, J.C., Millam, J.M., Iyengar, S.S., Tomasi, J., Barone, V., Mennucci, B., Cossi, M., Scalmani, G., Rega, N., Petersson, G.A., Nakatsuji, H., Hada, M., Ehara, M., Toyota, K., Fukuda, R., Hasegawa, J., Ishida, M., Nakajima, T., Honda, Y., Kitao, O., Nakai, H., Klene, M., Li, X., Knox, J.E., Hratchian, H.P., Cross, J.B., Adamo, C., Jaramillo, J., Gomperts, R., Stratmann, R.E., Yazyev, O., Austin, A.J., Cammi, R., Pomelli, C., Ochterski, J.W., Ayala, P.Y., Morokuma, K., Voth, G.A., Salvador, P., Dannenberg, J.J., Zakrzewski, V.G., Dapprich, S., Daniels, A.D., Strain, M.C., Farkas, O., Malick, D.K., Rabuck, A.D., Raghavachari, K., Foresman, J.B., Ortiz, J.V., Cui, Q., Baboul, A.G., Clifford, S., Cioslowski, J., Stefanov, B.B., Liu, G., Liashenko, A., Piskorz, P., Komaromi, I., Martin, R.L., Fox, D.J., Keith, T., Al-Laham, M.A., Peng, C.Y., Nanayakkara, A., Challacombe, M., Gill, P.M.W., Johnson, B., Chen, W., Wong, M.W., Gonzalez, C., Pople, J.A., 2003. Gaussian03. Gaussian Inc., Pittsburg, PA.

Guo, L., Meng, M., Zha, Y., 2006. Adsorption and thermal condensation of L-α-glutamic acid on Al_2O_3. Cuihua Xuebao 27, 189–194.

Harada, K., Fox, S.W., 1958. The thermal condensation of glutamic acid and glycine to linear peptides. Journal of the American Chemical Society 80, 2694–2697.

Hartmann, J., Christel Brand, M., Dose, K., 1981. Formation of specific amino acid sequences during thermal polymerization of amino acids. Biosystems 13, 141–147.

Henning, T., Begemann, B., Mutschke, H., Dorschner, J., 1995. Optical properties of oxide dust grains. Astronomy and Astrophysics Supplement Series 112, 143–149.

Kawamura, K., Takeya, H., Kushibe, T., 2009. Effect of condensation agents and minerals for oligopeptide formation under mild and hydrothermal conditions in related to chemical evolution of proteins. Advances in Space Research 44, 267–275.

Kumar, S., Rai, A.K., Singh, V.B., Rai, S.B., 2005. Vibrational spectrum of glycine molecule. Spectrochimica Acta Part A 61, 2741–2746.

Lagos, R., Baeza, M., Corsini, G., Hetz, C., Strahsburger, E., Castillo, J.A., Vergara, C., Monasterio, O., 2001. Structure, organization and characterization of the gene cluster involved in the production of microcin E492, a channel-forming bacteriocin. Molecular Microbiology 42, 229–243.

Lambert, J.F., 2008. Adsorption and polymerization of amino acids on mineral surfaces: a review. Origins of Life And Evolution of the Biosphere 38, 211–242.

Mandal, A.K., Balaram, P., 2007. Mass spectrometric identification of pyroglutamic acid in peptides following selective hydrolysis. Analytical Biochemistry 370, 118–120.

Martinez-Meeler, M., Aljinovic, N., Swain, D., 2003. Simple recipes of prebiotic soup. A high school or undergraduate chemistry laboratory. Journal of Chemical Education 80, 665–667.

Meng, M., Stievano, L., Lambert, J.F., 2004. Adsorption and thermal condensation mechanisms of amino acids on oxide supports 1. Glycine on silica. Langmuir 20, 914–923.

Miller, S.L., 1955. Production of some organic compounds under possible primitive earth conditions. Journal of the American Chemical Society 77, 2351–2361.

Mosqueira, F.G., Ramos-Bernal, S., Negrón-Mendoza, A., 2008. Prebiotic thermal polymerization of crystals of amino acids via the diketopiperazine reaction. Biosystems 91, 195–200.

Napier, J., Yin, J., 2006. Formation of peptides in the dry state. Peptides 27, 607–610.

Nittler, L.R., Alexander, C.M.O'D., Wang, J., Gao, X., 1998. Meteoritic oxide grain from supernova found. Nature 393, 222.

Panday, S.K., Prasad, J., Dikshit, D.K., 2009. Pyroglutamic acid: a unique chiral synthon. Tetrahedron: Asymmetry 20, 1581–1632.

Parrish, D.A., Mathias, L.J., 2002. Five- and six-membered ring opening of pyroglutamic diketopiperazine. Journal of Organic Chemistry 67, 1820–1826.
Pearson, J.F., Slifkin, M.A., 1972. The infrared spectra of amino acids and dipeptides. Spectrochimica Acta 28A, 2408–2417.
Peica, N., Lehene, C., Leopold, N., Schlülcker, S., Kiefer, W., 2007. Monosodium glutamate in its anhydrous and monohydrate form: differentiation by Raman spectroscopies and density functional calculations. Spectrochimica Acta Part A 66, 604–615.
Plankensteiner, K., Righi, A., Rode, B.M., Gargallo, R., Jaumot, J., Tauler, R., 2004. Indications towards a stereoselectivity of the salt-induced peptide formation reaction. Inorganic Chimica Acta 357, 649–656.
Righetti, B., Tamba, M., 1982. Infrared studies on the thermal degradation of DL-glutamic acid. Spectrochimica Acta 38, 57–60.
Rode, B.M.S., Suwannachot, H.L., Bujdak, Y.J., 1999. The combination of salt induced peptide formation reaction and clay catalysis: a way to higher peptides under primitive earth conditions. Origins of Life and Evolution of the Biosphere 29, 273–286.
Rohlfing, D.L., MacAlhaney, W.W., 1976. The thermal polymerization of amino acids in the presence of sand. Biosystems 8, 139–145.
Schoonen, M., Smirnov, A., Cohn, C., 2004. A perspective on the role of minerals in prebiotic synthesis. Ambio 33, 539–551.
Schwartz, A.W., 1996. Did minerals perform prebiotic combinatorial chemistry? Chemistry and Biology 3, 515–518.
Simoneit, B.R.T., 2004. Prebiotic organic synthesis under hydrothermal conditions: an overview. Advances in Space Research 33, 88–94.
Socrates, G., 2000. Infrared and Raman Characteristic Group Frequencies. Tables and Charts. John Wiley and Sons Ltd., Chichester.
Soloshonok, V.A., Ueki, H., Ellis, T.K., Yamada, T., Ohfune, Y., 2005. Application of modular nucleophilic glycine equivalents for truly practical asymmetric synthesis of β-substituted pyroglutamic acids. Tetrahedron Letters 46, 1107–1110.
Vijay, A., Sathyanarayana, D.N., 1992. Theoretical study of the ground-state vibrations of nonionized glycine. Journal of Physical Chemistry 96, 10735–10739.
Zhao, B., Wang, C., Zhao, S., Qin, M., Zhou, Z., Sun, Y., 2008. Density functional theory study on the structure and vibrational frequencies of glycylglycine. Spectrochimica Acta Part A 70, 301–306.